applied sciences

MDPI

Article

Functionalization Strategies and Fabrication of Solvent-Cast PLLA for Bioresorbable Stents

Romain Schieber [1,2,3], Yago Raymond [1,2,3], Cristina Caparrós [1], Jordi Bou [4], Enrique Herrero Acero [5], Georg M. Guebitz [5,6], Cristina Canal [1,2,3] and Marta Pegueroles [1,2,3,*]

1 Biomaterials, Biomechanics and Tissue Engineering Group, Department of Materials Science and Engineering, Technical University of Catalonia (UPC), EEBE, Av. Eduard Maristany, 10-14, 08019 Barcelona, Spain; romain.schieber@upc.edu (R.S.); santiago.raymond@mimetis.com (Y.R.); cristinacaparros@gmail.com (C.C.); cristina.canal@upc.edu (C.C.)
2 Barcelona Research Center in Multiscale Science and Engineering, Technical University of Catalonia (UPC), Av. Eduard Maristany, 10-14, 08019 Barcelona, Spain
3 Research Centre for Biomedical Engineering (CREB), UPC, 08019 Barcelona, Spain
4 Department of Chemical Engineering, Technical University of Catalonia (UPC), 08028 Barcelona, Spain; jordi.bou@upc.edu
5 Austrian Centre of Industrial Biotechnology, Konrad-Lorenz-Straße 20, 3430 Tulln an der Donau, Austria; enrique.herreroacero@acib.at (E.H.A.); guebitz@boku.ac.at (G.M.G.)
6 Institute of Environmental Biotechnology, BOKU—University of Natural Resources and Life Sciences Vienna, Konrad-Lorenz-Straße 20, 3430 Tulln an der Donau, Austria
* Correspondence: marta.pegueroles@upc.edu; Tel.: +34-934-054-154

Abstract: Actual polymer bioresorbable stents (BRS) generate a risk of device thrombosis as a consequence of the incomplete endothelialization after stent implantation. The material-tissue interactions are not fully controlled and stent fabrication techniques do not allow personalized medical solutions. This work investigates the effect of different functionalization strategies onto solvent-cast poly(L-lactic acid) (PLLA) surfaces with the capacity to enhance surface endothelial adhesion and the fabrication of 3D printed BRS. PLLA films were obtained by solvent casting and treated thermally to increase mechanical properties. Surface functionalization was performed by oxygen plasma (OP), sodium hydroxide (SH) etching, or cutinase enzyme (ET) hydrolysis, generating hydroxyl and carboxyl groups. A higher amount of carboxyl and hydroxyl groups was determined on OP and ET compared to the SH surfaces, as determined by contact angle and X-ray photoelectron spectroscopy (XPS). Endothelial cells (ECs) adhesion and spreading was higher on OP and ET functionalized surfaces correlated with the increase of functional groups without affecting the degradation. To verify the feasibility of the approach proposed, 3D printed PLLA BRS stents were produced by the solvent-cast direct writing technique.

Keywords: poly(L-lactic acid) solvent casting; surface modification; cold atmospheric plasma; cutinase enzyme; biocompatibility; 3D printed stent

check for updates

Citation: Schieber, R.; Raymond, Y.; Caparrós, C.; Bou, J.; Herrero Acero, E.; Guebitz, G.M.; Canal, C.; Pegueroles, M. Functionalization Strategies and Fabrication of Solvent-Cast PLLA for Bioresorbable Stents. *Appl. Sci.* **2021**, *11*, 1478. https://doi.org/10.3390/app11041478

Academic Editor: Giuseppe Perale
Received: 5 December 2020
Accepted: 1 February 2021
Published: 6 February 2021

1. Introduction

In the cardiovascular field, in-stent restenosis (ISR) and late stent thrombosis (LST) are the main complications after stent implantation mainly due to a non-controlled and non-specific biological response of endothelial cells (ECs), smooth muscle cells (SMCs), and platelets to the stent surface [1]. Bioresorbable stents (BRS) were recently developed to decrease the rate of LST by reducing the exposure time of the stent surface to the blood flow [2,3]. Bioresorbable polymers from the family of aliphatic poly(esters) degrade in situ by hydrolysis and the degradation products are metabolized by the organism itself. Poly(lactic acid) and its copolymers are a class of bioresorbable, biocompatible, and FDA approved biomaterial, in which mechanical, easy-of-fabrication, and degradability properties make them among the most often used polymers for the biomedical applications [4,5].

Ideally, poly(L-lactic acid) (PLLA) stents should maintain the artery widely open during the first months following implantation, are expected to degrade in a controlled manner and, finally, heal the vessel and restore the physiological function of the artery [6]. However, current PLLA BRS fail to reduce ISR and LST [7–9]. A strategy to reduce this complication could be to design new BRS surfaces that enhance re-endothelialization [10].

Surface modifications onto biomaterials are a common approach to control the biological response and can be classified into three main categories. First, topographical modifications that obtain specific nano- or micro-patterned surfaces can accelerate ECs migration [10,11]. Second, physico-chemical modifications that generate suitable functional groups [12,13] and/or modulate surface energy [14,15] have demonstrated to modify ECs adhesion and spreading. Third, surface biofunctionalization by immobilizing specific biomolecules derived from extracellular matrix (ECM) proteins that have selectivity for ECs, could facilitate a cascade of biological events and eventually regenerate the damaged area with a functional endothelium [16–18]. A strong covalent bonding between the implant and the biomolecules is desired to obtain a stable biofunctionalization [19]. The most common chemical routes to obtain covalent bonding are the generation of functional groups at the surface, generally carboxyl (-COOH) or hydroxyl (-OH) groups, which react with a specific part of the biomolecule. Consequently, modifications that increase surface implant functional groups are of double interest since they can increase biocompatibility and enhance biofunctionalization. In that sense, surface treatments such as cold plasma treatment [20–22], ultraviolet irradiation [12], sodium hydroxide (NaOH) etching [23,24], or ozone irradiation [13] have shown to ameliorate surface functionalization. Moreover, enzymatic treatments have been proposed and successfully used for the surface modification of natural and synthetic polymers [18,25]. For polyesters, such as PLLA, the hydrolysis of the ester bond by applying cutinase enzymes generates new hydroxyl and carboxyl groups on the surface, which have been used to direct drug loading [26] or to bind serum albumin in order to increase biocompatibility [18]. Different activation treatments work differently on PLLA surfaces. While the NaOH treatment is a more aggressive non-selective hydrolysis that etches the surface [27,28], oxygen plasma acts more superficially (some nanometers) and, depending on the treatment conditions, it can generate non-specific functionalization, hydrolysis and, eventually, etching [29,30]. The cutinase enzyme allows a selective hydrolysis of the ester bonds of the outermost surface layers of the polymer (<100 nm), generating only hydroxyl and carboxyl groups [27,31].

Furthermore, common stent fabrication processes do not allow personalizing the stent shape. Consequently, in complex arteries stent implantation is impossible. Three-dimensional printing could be a strategy to produce stents with a shape fully customized to the damaged artery. In particular, the solvent-cast direct writing technique has shown promising results to obtain complex 3D-printed shapes with PLLA inks [32].

The aim of this work was to design and characterize solvent-casted PLLA functionalized surfaces to enhance ECs adhesion and to assess the use of this process and biomaterial to fabricate the 3D-printed BRS. To assess biocompatibility, mechanical and degradation properties of the solvent-cast PLLA films, the cytotoxicity, crystallinity, molecular weight, Young's modulus, ultimate tensile strength (UTS), and degradation rates were evaluated. The effect of the three different functionalization processes on PLLA properties was compared by characterizing surface roughness, surface wettability, degradation of films, surface chemical properties, and ECs adhesion. Finally, to assess its feasibility, 3D printed PLLA bioresorbable stents were obtained by the solvent-cast direct writing technique.

2. Materials and Methods

2.1. Materials

Medical grade poly-L-lactic acid (PLLA) pellets (PURASORB PL65, $M_w \approx 1{,}650{,}000$ g/mol, 51% crystallinity) were obtained from Purac Biomaterials (Gorinchem, Netherlands). PLLA pellets were stored in a desiccator at room temperature (RT).

The biodegradable PLLA peripheral stent REMEDY (Kyoto Medical Planning, Japan) was used in this study as a positive control.

The Humicola insolens cutinase enzyme (HiC) was kindly provided by Novozymes (Beijing, China) and used as received without any purification steps.

Human umbilical vein endothelial cells (HUVECs) (Lonza Group Ltd., Switzerland) were grown in an EC basal medium (EBM®) supplemented with 4% (*v*/*v*) fetal bovine serum (FBS), 0.1% (*v*/*v*) gentamicin sulphate amphotericin (GA-1000), 0.4% (*v*/*v*) recombinant human fibroblast growth factor (rhFGF), 0.1% (*v*/*v*) recombinant human epidermal growth factor (rhEGF), 0.1% (*v*/*v*) ascorbic acid, 0.1% (*v*/*v*) vascular endothelial growth factor (VEGF), 0.1% (*v*/*v*) recombinant Long R insulin (R3-IGF-1), and 0.04% (*v*/*v*) hydrocortisone (EBM and all supplements were obtained from Lonza). Cells were maintained at 37 °C, in a humidified atmosphere containing 5% (*v*/*v*) CO_2. The culture medium was changed every 2 days. The cell culture was performed in Nunc cell flasks (Thermo Scientific, Denmark) in a completed medium. Upon reaching 70% confluence, cells were detached by trypsin/EDTA (Sigma-Aldrich), centrifuged, and subcultured into a new flask or re-suspended in a serum-free medium and used for cell assays. All the experiments were conducted using HUVECs at passages 4 to 6 [33,34].

2.2. Synthesis of PLLA Films by Solvent Casting

The PLLA films were obtained by the solvent-casting method [35]. Previously, PLLA pellets were dried in an oven with a controlled argon atmosphere at 80 °C for 2 h. Then, PLLA pellets were dissolved in chloroform (Sigma-Aldrich, Germany) at a 3.6% weight versus volume (*w*/*v*) ratio. The dissolution took approximately 48 h on an orbital shaker at RT. Once the PLLA was completely dissolved, the obtained paste was spread on a 150 mm diameter glass petri dish and maintained 48 h under a chloroform saturated atmosphere to decrease the solvent evaporation rate. The studied surface was the one in contact with the glass petri dish. The obtained films had a thickness of approximately ≈ 150 µm. The obtained solvent casting films were coded as SC. To increase crystallinity, the films were thermally treated at 80 °C during 12 h and coded as TT. Finally, to characterize the films, they were cut into 10 mm diameter discs.

2.3. Surface Functionalization of PLLA Films

Three different techniques of surface functionalization were applied to the fabricated TT films:

- **Oxygen plasma:** Low-pressure oxygen plasma was generated in a 13.56 MHz radiofrequency reactor Diener Femto (Diener, Germany). TT films were treated in the center of the reactor. The oxygen plasma was generated at 0.4 mbar pressure and 100 W discharge power during 2 min. Details on the experimental setting can be found in a previous study [36]. The obtained samples were coded as OP.
- **Sodium hydroxide etching:** TT films were chemically activated by submerging the samples in a 1 M sodium hydroxide (NaOH) solution under sonication during 1 h at RT. Subsequently, the treated samples were cleaned twice in distilled water for 30 min to remove NaOH residues and the samples were coded as SH.
- **Enzyme treatment:** Previously to the cutinase enzymes activation, TT films were prewashed as described in a previous study [31]. Briefly, samples were submerged successively in L-1 Triton X100, Na_2CO_3 solution, and double-distilled water (ddH_2O) for 30 min at 37 °C and 130 rpm. Afterwards, cutinase enzymes were diluted in 100 mM Tris-HCl buffer with a pH value of 7 to obtain a 10 µM enzyme solution. The films were immersed in 1 mL of the enzyme solution at 37 °C on an orbital shaker at 100 rpm during 24 h. Finally, the films were cleaned with the previous protocol and the obtained samples were coded as ET.

2.4. Characterization of PLLA Films

Gel permeation chromatography (GPC) analyses were performed in an Agilent HPLC chromatograph 1260 Infinity series (Agilent Technologies, Santa Clara, CA, USA). The separation was carried in a Waters Styragel HR 5E column (USA) using $CHCl_3$ (HPLC grade) as an eluent. The samples with a concentration between 0.2 to 0.4 mg/mL were analyzed. The used flow was 0.4 mL/min and the amount of injected samples was 20 µL. Molecular weights were calculated after calibration with PMMA standards from Sigma-Aldrich (Darmstadt, Germany), the molecular weight calibration range was between 2.7 million to 2000 Dalton. The calculations were performed with the Chemstation Software (Agilent Technologies).

The crystalline properties of the different PLLA samples were analyzed by differential scanning calorimetry (DSC) with the instrument DSC 2920 Modulated (TA Instruments, USA) and following the ASTM D3418-03 standard [37]. An empty aluminum pan was used as a reference. Ten milligrams of the samples were run in a nitrogen atmosphere at 10 °C·min^{-1} heating ramp from 20 to 220 °C. The enthalpy of fusion (ΔHm) and the enthalpy of crystallization (ΔHcc) were obtained from the scan and used to calculate the percentage of crystallinity through the equation Xc = (ΔHm − ΔHcc)/ΔH^0m, where ΔH^0m = 93 J/g is the enthalpy of fusion of a 100% crystalline PLLA [38,39].

The mechanical properties of the PLLA films were determined by the tensile test (DY 34, Adamel Lhomargy, France) according to the standard ASTM D882-02 [40] using a 100 N load cell. First, PLLA films were cut following the standard ASTM D6287-98 [41] to obtain five samples of 150 mm length and 10 mm width for each studied condition. The rate of grip separation was set to 15 mm/min and the curve load versus the extension was recorded at RT. From the curve, Young's modulus (E) and the ultimate tensile strength (UTS) were obtained.

To detect residues of chloroform in the PLLA films, the energy-dispersive X-ray spectroscopy (EDX) was performed with a Zeiss Neon40 FE-SEM microscope (Carl Zeiss NTS GmbH, Germany). Five measurements at 7 kV were done for each condition.

The indirect in vitro cell cytotoxicity of the PLLA films was evaluated from extracts using the lactate dehydrogenase (LDH) enzyme measurement on HUVECs. The extracts were prepared according to ISO 10993-5 [42] by submerging the different fabricated PLLA films in a complete cell medium for 3 days at 37 °C. Then, the extracts were serially diluted into five concentrations as 1/1; 1/2; 1/10; 1/100, and 1/1000 with a fresh complete cell medium. Previously, PLLA films were sterilized in ethanol 70% during 30 min. The cells were seeded in a 96-well tissue polystyrene (TCPS) cell culture plate at a seeding density of 15,000 HUVECs/well and incubated normally for 24 h to allow an attachment. Afterwards, the cell medium was replaced by 200 µL of the different extract dissolutions. A complete fresh medium was used as a negative control and a complete fresh medium without cells was used as a positive control. After 24 h, alive HUVECs were quantified by measuring the LDH enzyme. Briefly, the cells were rinsed with PBS and lysed with 350 µL of the mammalian protein extraction reagent (M-PER) (Thermo Scientific, Darmstadt, Germany). The activity of LDH was determined by measuring the spectrophotometrical absorbance with a commercial LDH kit (Cytotoxicity Detection Kit, Roche Diagnostics, Manheim, Germany) by a microplate reader (Infinite M200 PRO, Tecan Group Ltd., Switzerland) at 490 nm. According to the standard, cell viability was calculated with the following equation: Cell viability = $(Abs_{sample} - Abs_{C+}/(Abs_{C-} - Abs_{C+})$ where Abs_{sample} is the sample absorbance, Abs_{C+} is the positive control absorbance, and Abs_{C-} is the negative control absorbance. The results were shown by the percentages. Morphological signs of cell death were visible when the values of cell survival were below the level of 80%, which was referred to as a threshold to define a cytotoxic response.

2.5. Surface Characterization

Topography was evaluated with white light interferometry (WLI) (Optical interferometer Veeco Wyko 9300NT, Veeco Instruments, Plainview, NY, USA) in a vertical scanning

interferometry mode (VSI) at 100× magnification. Data analysis was performed with the Wyko Vision 4.10 software (Veeco Instruments) to obtain the roughness parameter Ra (the arithmetic average height). The curvature and tilt were eliminated with a Gaussian filter.

The water static contact angle was measured by the sessile drop method with a Contact Angle System OCA15plus (Dataphysics, Filderstadt, Germany) [43]. Milli-Q® water drops of 3 µL were deposited on the PLLA films and the contact angle between the water and different PLLA films was measured. An average of 15 drops was studied for each condition. The contact angle values were obtained after applying Laplace-Young fitting of the drop profile with the SCA 20 software (Dataphysics). For roughness and wettability results, three biological replicas, each of them with three technical replicates, were performed.

The chemical composition of the surface of PLLA films before and after topographical modification was analyzed by X-ray photoelectron spectroscopy (XPS) (SPECS Surface NanoAnalysis GmbH, Berlin, Germany). The XPS spectra were obtained using an Mg anode XR50 operating at 150 W and a Phoibos 150 MCD-9 detector to record high-resolution spectra at a pressure below 7.5×10^{-9} mbar. The elements present on the surface were evaluated by low-resolution survey spectra, whereas a high-resolution of C 1s was recorded with a detector pass energy fixed at 25 eV with 0.1 eV step at a pressure below 7.5×10^{-9} mbar. The Casa XPS software (version 2.3.16, Casa Software Ltd., Teignmouth, UK) was used to do fitting, peak integration of spectra, and peaks deconvolution. Binding energies were referred to the C-C bond energy at 284.8 eV.

2.6. PLLA Films Degradation

To compare the rate of degradation of the different PLLA films compared to the REMEDY stent, an accelerated degradation assay was performed in an alkaline solution [28,44,45]. First, in order to have the same ratio surface/volume for each condition, all the PLLA films were cut in rectangular fibers with sections similar to REMEDY stent strut sections (≈70,000 μm^2). All the initial samples (REMEDY stent, SC, TT, OP, SH, and ET) were dried in an argon atmosphere oven at 48 °C during 2 h and weighed with a Sartorius Quintix35-1S laboratory balance (Göttingen, Germany). Next, all the samples were placed at 37 °C in a 100 mL solution of 0.1 M NaOH. At 2, 4, 7, and 10-days, the samples were dried as initially (at 48 °C during 2 h) and weighed in order to calculate the mass loss. Moreover, initial and final samples surfaces were observed by scanning electron microscopy (SEM) with a Zeiss Neon40 FE-SEM microscope (Carl Zeiss NTS GmbH, Oberkochen, Germany). For each sample, five images were taken at a working distance of 6 mm and a potential of 5 kV. Finally, the samples topography was characterized by WLI, as previously described (Section 2.5), to evaluate changes between the final (Ra_f) and initial (Ra_i) mean roughness, the ratio Ra_f/Ra_i was calculated.

2.7. HUVECs Adhesion

The cell adhesion assay was performed by seeding HUVEC at a density of 5×10^4 cells/sample with a serum-free medium and cellular analyses were carried out at 12 h after cell seeding. The different PLLA samples were previously sterilized in ethanol 70% during 15 min at RT. To quantify the density of adhered HUVECs after 12 h, the release of the LDH enzyme was measured as previously described for the indirect cytotoxicity assay (Section 2.4) and, in parallel, cell adhesion was observed by SEM. To that end, HUVECs were fixed with glutaraldehyde (G400-4, Sigma-Aldrich), dehydrated by immersion in different solutions of increasing ethanol% and, finally, sputtered with a gold-palladium coating. For each sample, ten images were taken at a working distance of 6 mm and a potential of 5 kV. The percentage of area covered by HUVEC was determined using the FIJI ImageJ software [46].

2.8. 3D Printed BRS Obtained by the Solvent-Cast Direct Write Technique

The 3D printed PLLA stents were obtained using a BCN 3D+ printer (BCN 3D technologies, Barcelona, Spain). The printer was modified to solvent cast PLLA inks through a syringe micro-nozzle with a 250 µm inner diameter (Nordson®, Carlsbad, CA, USA). PLLA

inks were prepared as described in Section 2.2 and printing was performed at a 0.4 $mm^3 \cdot s^{-1}$ flux and 4 $mm \cdot s^{-1}$ robot velocity. Moreover, the printer Y-axis was modified by introducing a carbon fiber rotating mandrel in order to print cylindrical structures. The BRS shape was inspired by the Igaki-Tamai stent (Kyoto Medical Planning, Japan) design structure and its dimensions were 5 mm diameter and 20 mm length. The software CATIA (Dassault Systèmes, France) was used for the stent design and the resulting Computer-Aided Design part was exported to the STL format. Finally, Slic3r (open source) was used to translate STL to G-code, which was needed for the 3D printer.

2.9. Statistical Analysis

The experimental data collected in this study are reported as the mean ± standard deviation. A one-way analysis of variance (ANOVA) was used to determine the statistical significance of difference at $p < 0.05$ (Minitab 16.2.2 Statistical Software, Minitab Inc., State College, PA, USA). Unless otherwise specified, all the experiments were performed with at least n = 3 samples for each specimen group. In addition, each experiment was repeated at least twice.

3. Results and Discussion

The aim of this study was to evaluate solvent-casted PLLA as a biomaterial for stent fabrication by 3D printing, and, its functionalization to enhance ECs adhesion. To this end, the effect of solvent casting and functionalization processes onto PLLA's biocompatibility, degradation and mechanical properties were evaluated. The generation of functional groups at the surface, generally carboxyl (-COOH) or hydroxyl (-OH) groups, can be obtained by different routes as explained in Figure 1. Two wet-processes involving chemical hydrolysis by sodium hydroxide (SH) or enzymatic treatment (ET) produces scission of the ester bonds in the chain generating new hydroxyl and carboxyl groups on the surface. In contrast, the oxygen plasma (OP) treatment, produces excited species in the gaseous phase (i.e., O* radicals, O^{2-} ions, etc.) with high reactivity that can graft new chemical groups to the polymer surface through a dry process. Therefore, the density of surface functional groups was measured to compare the effect of NaOH, oxygen plasma, and cutinase enzymes employed as surface activation treatments. Finally, as a proof of concept, 3D-printed PLLA stents were obtained by the solvent-cast direct-write technique.

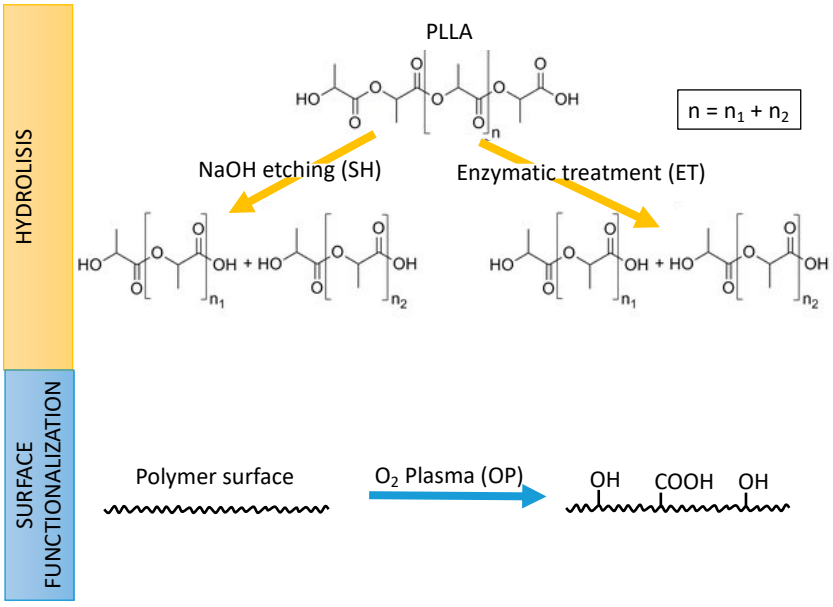

Figure 1. Strategies followed in this work for the generation of functional carboxyl (-COOH) or hydroxyl (-OH) onto poly(L-lactic acid) (PLLA): Hydrolysis by sodium hydroxide etching (SH) or enzymatic treatment (ET) (top); and surface functionalization by oxygen plasma (OP) (bottom).

3.1. PLLA Film Properties

To evaluate potential cytotoxic effects of the solvent employed for the synthesis of the PLLA films and/or the different activation treatments, an indirect cytotoxicity assay was performed (Table 1). The ISO 10993-5 standard specifies that a material is cytotoxic if the percentage of cell survival is inferior to 80%. The results indicated that SC samples were cytotoxic but the thermal treatment increased cell viability reaching non-cytotoxic values, higher than 92%, as observed for the TT samples at different dilutions. Activation treatments with oxygen plasma (OP) or enzymatic treatment (ET) did not affect the cytotoxicity of TT films. However, SH samples presented cytotoxicity in some cases probably due to NaOH residues in the obtained films.

Table 1. Cell viability on the different solvent-cast PLLA films. Results correspond to the percentage of living cells after an indirect cytotoxicity assay. Extracts were obtained by submerging the different fabricated PLLA films in a complete cell medium for 72 h. The extracts were serially diluted 1/1, 1/2, 1/10, 1/100, 1/1000 with a fresh complete cell medium. Values < 80% indicate human umbilical vein endothelial cells (HUVEC) cytotoxic surfaces. **SC**: Solvent casting PLLA films; **TT**: Thermally treated SC films; **OP**: Oxygen plasma TT films; **SH**: Sodium hydroxide etched TT films; **ET**: Enzyme treated TT films.

	Cell Viability (%)				
Sample	**1/1**	**1/2**	**1/10**	**1/100**	**1/1000**
SC	45 ± 26	70 ± 13	67 ± 12	79 ± 16	94 ± 12
TT	95 ± 3	95 ± 4	92 ± 4	102 ± 15	96 ± 7
OP	101 ± 4	113 ± 6	122 ± 16	116 ± 12	113 ± 18
SH	95 ± 15	92 ± 19	76 ± 12	86 ± 7	123 ± 13
ET	98 ± 11	112 ± 24	111 ± 25	112 ± 12	121 ± 21

The presence of chlorine residues from solvent casting fabrication was verified by EDS (Table 2). SC was the only film presenting chlorine residues. As chloroform toxicity is well known [47,48], the cytotoxicity of SC observed previously was probably due to this residual chloroform in the film. Moreover, the absence of chlorine in TT films suggested that the thermal treatment helped PLLA solvent-cast films to be biocompatible by evaporating chloroform residues.

Table 2. Bulk properties of the commercial REMEDY stent and all the different solvent-cast films: Presence of chloride (Cl) residues, Mw: Molecular weight obtained by HPLC and % of crystallinity following DSC. **SC**: Solvent casting PLLA films; **TT**: Thermally treated SC films; **OP**: Oxygen plasma TT films; **SH**: Sodium hydroxide etched TT films; **ET**: Enzyme treated TT films.

Sample	**Cl Residues**	**Mw (10^6 g/mol)**	**% Crystallinity**
REMEDY stent	No	0.19 ± 0.00	50.5 ± 2.7
SC	Yes	0.95 ± 0.04	12.5 ± 3.1
TT	No	0.98 ± 0.03	26.6 ± 2.7
OP	No	0.95 ± 0.01	25.1 ± 1.7
SH	No	0.89 ± 0.01	24.2 ± 2.7
ET	No	0.97 ± 0.02	25.8 ± 0.4

PLLA PL65 from Purac was chosen for its particularly high molecular weight and crystallinity in order to fabricate PLLA films with mechanical and degradation properties similar to the actual commercial PLLA BRS. The potential reduction in molecular weight and crystallinity due to solvent casting were investigated by GPC and DSC (Table 2). Generally, all the processed films presented M_w values in the same range, from 0.89 up to 0.98 × 10^6 g/mol. The REMEDY stent presented a M_w five times lower than SC films. SC and TT films presented a statistically similar molecular weight of 0.95 ± 0.04 and 0.98 ± 0.03 10^6 g/mol, respectively. Therefore, the thermal treatment did not significantly

affect the PLLA chain length: Nor by generating polymerization, neither by degrading PLLA. The three functionalizing treatments could break the PLLA chains and, consequently, reduce the PLLA films M_w. No significant changes were observed after plasma activation (OP) and enzyme hydrolysis (ET) suggesting that these processes work at the outermost surface layer. On the contrary, SH showed a significant 10% reduction of the molecular weight compared to TT meaning the NaOH etching affects a deeper surface layer compared to the other treatments.

A huge difference in crystallinity is observed between the REMEDY stent, 50.5 ± 2.7%, and the processed films, results are below 26% (Table 2). The SC films presented a percentage of crystallinity four times lower than the PL65 pellet employed for its synthesis. This decrease of crystallinity due to the solvent casting process has already been reported [49] and is mainly associated with the fast chloroform evaporation not allowing polymer macromolecules to diffuse to the crystal growth front and overcome the energy barrier of deposition [50]. As expected, the thermal treatment helped increase crystallinity, which doubled in TT due to the chain reorganization [45,51]. Moreover, the three activation treatments did not affect crystallinity.

A tensile test was done on SC and TT to evaluate the effect of the thermal treatment on mechanical properties. TT films presented a five times higher Young's modulus (2.85 ± 0.27 GPa) and two times higher UTS (62.2 ± 5.7 MPa) compared to the SC films (E: 0.53 ± 0.10 GPa and UTS: 28.9 ± 2.6 MPa). The increased mechanical properties on TT films are related to their increased crystallinity [52] and the evaporation of solvent residues was produced by the thermal treatment. Indeed, solvent residues act as a plasticizer and dramatically reduce the tensile strength [49]. The Young's modulus and UTS of the TT films are in the upper range of the mechanical properties reported for the PLLA family [53]. This allows inferring that the obtained solvent-cast PLLA would probably respond properly to the mechanical stress occurring during the stent implantation, justifying the interest of obtaining 3D printed PLLA biodegradable stents by the solvent casting direct writing technique [32].

3.2. Surface Characterization

Surface roughness modifications due to the activation treatments were characterized by white light interferometry (WLI) (Figure 2a). SC surfaces displayed the lowest value of R_a, but it was statistically equal to TT, OP, and ET suggesting that these three treatments had a negligible effect on the surface roughness. Contrarily, the effect of NaOH treatment was more aggressive and modified the surface roughness parameters by doubling the parameter Ra compared to the other films. In addition to the fact that the NaOH treatment also decreased the PLLA molecular weight, it is evidenced that the alkaline activation process was a more aggressive treatment than the plasma or enzymatic treatment, affecting a few microns depth from the surface of PLLA films.

The wettability of the different fabricated PLLA films was characterized by a water contact angle (Figure 2b). Moreover, the wettability evaluation revealed that the thermal treatment significantly increased the water contact angle compared to SC. This difference could be explained by the higher crystallinity of TT films, inducing a lower percentage of amorphous phase groups and, consequently, lower hydrophilicity. On the one hand, NaOH etching did not change the wettability as SH presented a water contact angle of 84.2 ± 4.3° with no-statistical differences when compared to TT. On the other hand, plasma and enzyme activation treatments significantly reduced the water contact angle, obtaining values ≈20° and ≈25° lower than TT, respectively. Other authors have already reported the increase in hydrophilicity after the plasma treatment and enzymatic hydrolysis [31,54–56] on PLA, or other polyesters. This is usually attributed to the generation of new surface functional groups [22,55,57].

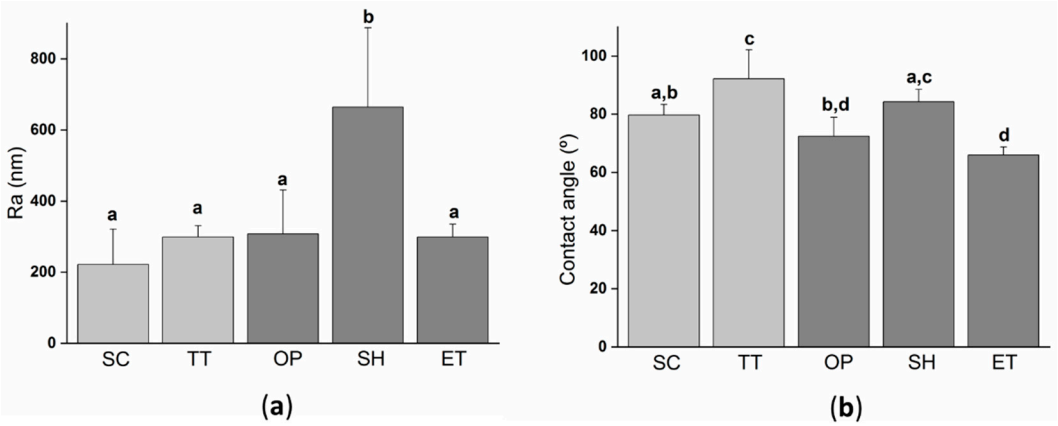

Figure 2. Surface properties of the solvent-cast PLLA films submitted to different treatments: (**a**) Roughness Ra (arithmetic roughness average) calculated from white light interferometry (WLI) images; (**b**) water contact angle on the different PLLA films. Columns marked with different letters belong to statistically different groups (p-value < 0.05). **SC**: Solvent casting PLLA films; **TT**: Thermally treated SC films; **OP**: Oxygen plasma TT films; **SH**: Sodium hydroxide etched TT films; **ET**: Enzyme treated TT films.

The surface chemical composition of TT and activated films is shown in Table 3. The XPS analysis revealed the presence of C 1s, O 1s, N 1s, and Na 1s.

Table 3. Analysis of the atomic composition percentage at the TT, OP, SH, and ET surfaces by XPS. The elemental composition of O 1s, C 1s, N 1s, Na 1s, and the ratio between O/C were obtained from the XPS survey spectra. Values of the relative chemical carbon bonds were obtained from the deconvolution of C 1s peaks. **TT**: Thermally treated films; **OP**: Oxygen plasma TT films; **SH**: Sodium hydroxide etched TT films; **ET**: Enzyme treated TT films.

	Elemental Composition (Atomic %)					**Relative Chemical Carbon Bonds (%)**		
	O 1s	**C 1s**	**N 1s**	**Na 1s**	**O/C**	**284.7 eV C-C, C-H**	**286.6 eV C-O**	**288.8 eV O=C-O**
TT	37.7 ± 0.5	62.3 ± 0.5	0.0 ± 0.0	0.0 ± 0.0	0.61	42.1 ± 0.9	28.7 ± 0.7	29.2 ± 0.6
OP	42.3 ± 0.3	56.8 ± 0.4	0.8 ± 0.1	0.0 ± 0.0	0.75	30.4 ± 0.2	32.8 ± 0.1	36.9 ± 0.1
SH	39.0 ± 0.3	60.9 ± 0.2	0.0 ± 0.0	0.2 ± 0.0	0.64	34.6 ± 0.9	34.7 ± 1.4	30.7 ± 1.0
ET	49.0 ± 0.2	50.4 ± 0.2	0.5 ± 0.1	0.0 ± 0.0	0.97	31.1 ± 0.4	32.4 ± 0.6	36.6 ± 0.4

The atomic percentage of O 1s increased, while C 1s decreased for all the activated surfaces compared to TT films. Consequently, the O/C ratio was higher on the activated surfaces (>0.64) compared to TT (0.61). The increase confirmed the incorporation of O 1s on the PLLA film surfaces to form functional groups. The O/C ratio was statistically higher on OP and ET films, 0.75 and 0.97, respectively compared to SH (0.64), suggesting a higher efficiency of plasma and enzyme to create functional groups. Moreover, the presence of N 1s was observed in small quantities on OP and ET films 0.8 ± 0.1 and 0.5 ± 0.1%, respectively. For the OP samples, the detection of N 1s can be associated with air contaminations in the plasma chamber, while the ET samples can be ascribed to residues of cutinase, as cutinase contains nitrogen [58]. Finally, the SH films showed the presence of low amounts of Na 1s (0.5 ± 0.1%). These residues of NaOH could explain the cytotoxicity observed on these films.

The decomposition of the high-resolution C 1s peak of TT and the activated samples (Figure 3 and Table 3) revealed three peaks on all surfaces corresponding to: (1) C-C and C-H bonds at 284.7 eV; (2) C-O bonds at 286.6 eV; and (3) O = C-O bonds at 288.8 eV [56]. The surfaces with any of the three activation treatments presented a significantly higher atomic percentage of O = C-O bonds (>30.7 ± 1.0%) than TT films (29.2 ± 0.6%) indicating that all three activation treatments were able to create -COOH functional groups on the surface. Plasma and enzymatic treatments presented 36.9 ± 0.1 and 36.6 ± 0.4% of O = C-O bonds, respectively, meaning a higher amount of carboxyl groups were created

on these surfaces than on the alkaline surface (30.7 ± 1.0%). When hydrolyzing an ester bond, a single-COOH and a single -OH group are created [59]. As the NaOH solution and enzyme act on PLLA only by ester bond hydrolysis, on the SH and ET surfaces the increase of hydroxyl groups is proportional to the increase of the carboxyl groups. The plasma treatment does not act only by hydrolysis; there is also a grafting of new functional groups in the surface with the oxygen-excited species present in the plasma. The fact that the O/C ratio was inferior on OP compared to ET and that OP and ET presented a similar percentage of carboxyl groups suggested that OP had fewer hydroxyl groups than ET.

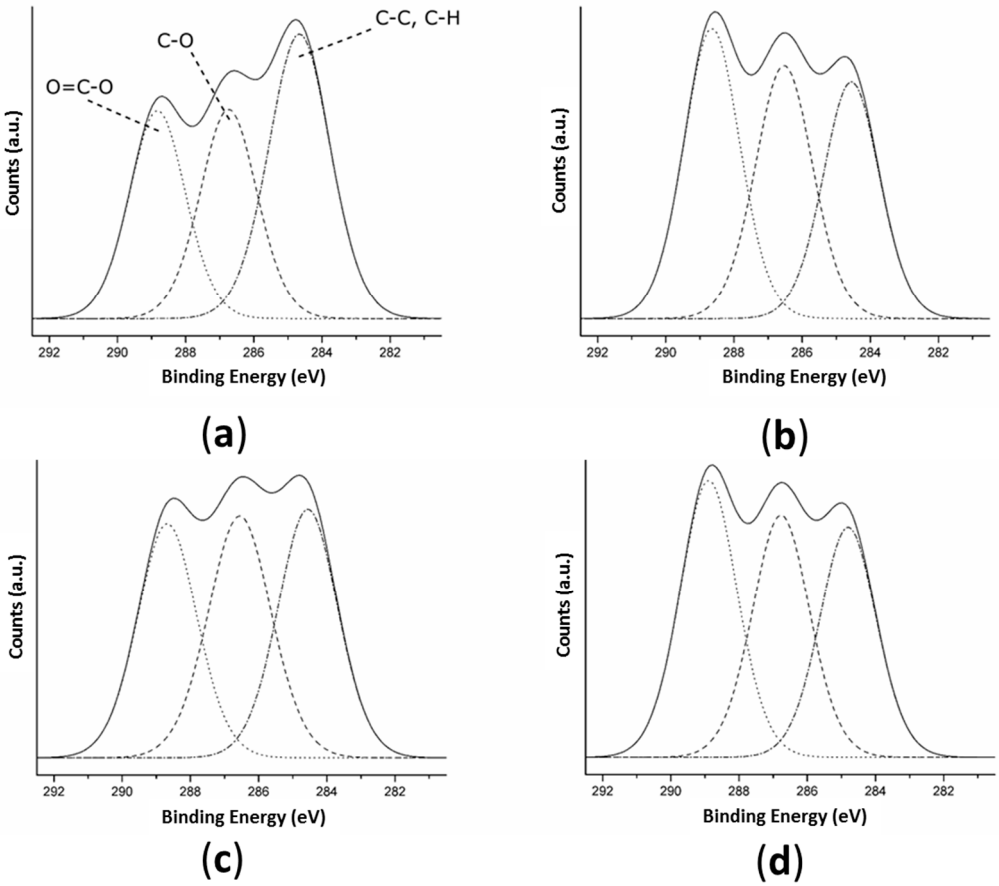

Figure 3. High-resolution spectra of C 1s obtained by XPS for: (**a**) TT; (**b**) OP; (**c**) SH; and (**d**) ET surfaces. Dashed lines represent the fitting components and the solid line represents the sum of these components. **TT**: Thermally treated films; **OP**: Oxygen plasma TT films; **SH**: Sodium hydroxide etched TT films; **ET**: Enzyme treated TT films.

The higher density of functional groups on OP and ET compared to the SH samples is coherent with the higher decrease of wettability observed after the plasma or enzyme hydrolysis compared to the alkaline hydrolysis, suggesting that the plasma and enzyme hydrolysis presented the best efficiency to create functional groups to the subsequently biofunctionalized surface or to improve the implant biological response.

3.3. Degradation of PLLA Films

BRS stents are expected to maintain their radial strength at least during the 6 months post-implantation, the stent material should degrade without losing mechanical properties during this period of time [60,61]. The high M_w PLLA are expected to have a slow degradation rate compared to the low M_w polyester [62]. An accelerated degradation assay was conducted in conditions similar to the previous works [28,44,45,63]. The films were immersed in a 0.1 M NaOH solution during 10 days in order to evaluate the effect of solvent-casting, thermal, and activation treatments on the degradation of high M_w PLLA by measuring the percentage of mass loss (Figure 4). Moreover, SEM images of the surface and

roughness measurement by WLI of the studied surfaces before and after the degradation assay are shown in Figure 5.

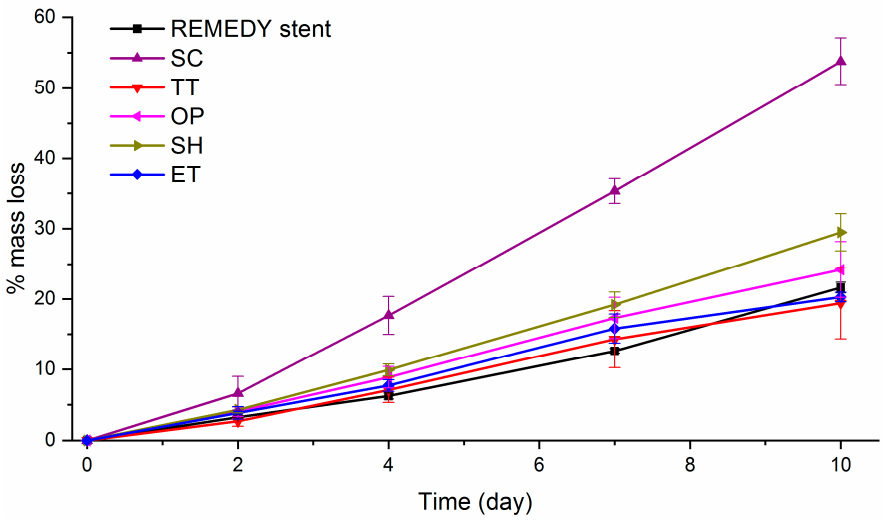

Figure 4. Percentage of mass loss evolution during the alkaline accelerated degradation assay on the REMEDY stent and all solvent-cast PLLA films. The assay was done in a 0.1 M NaOH solution during 10 days. **SC**: Solvent casting PLLA films; **TT**: Thermally treated SC films; **OP**: Oxygen plasma TT films; **SH**: Sodium hydroxide etched TT films; **ET**: Enzyme treated TT films.

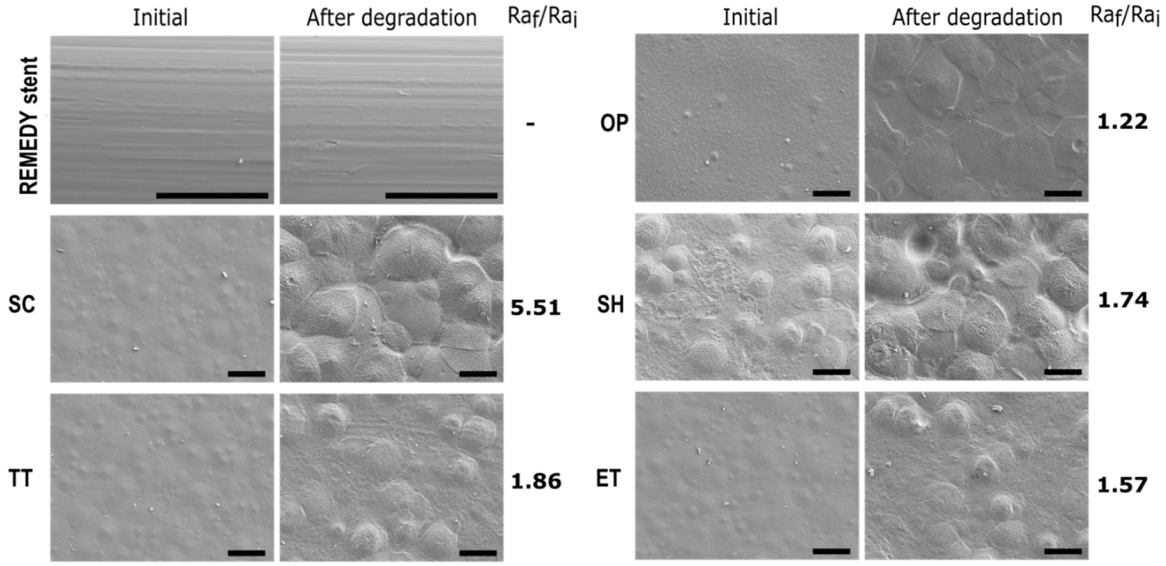

Figure 5. SEM images and roughness ratio Raf/Rai of the REMEDY stent and all solvent-cast PLLA films before and after the alkaline accelerated degradation assay. The assay was done in a 0.1 M NaOH solution during 10 days. Scale bar = 50 µm. Roughness was obtained from WLI. The REMEDY stent roughness could not be characterized for geometrical reasons. **SC**: Solvent casting PLLA films; **TT**: Thermally treated SC films; **OP**: Oxygen plasma TT films; **SH**: Sodium hydroxide etched TT films; **ET**: Enzyme treated TT films.

As expected, all the samples presented a quasi-linear decrease in the percentage of mass loss with time. This behavior, was already described by D. Cam et al. [44] in an alkaline solution and is completely different from the sigmoidal degradation pattern observed for PLLA in saline and buffered solutions or in body conditions related to Middleton et al. [61]. SC films clearly presented statistically significant faster degradation rates compared to the other surfaces. For example, the SC mass loss after 10 days was higher than 45%, whereas, all the other films had a mass loss lower than 30%. According to the literature [44], as

degradation occurs first in the amorphous parts of the polymer, the faster degradation on SC can be explained by the lower crystallinity of this film. In addition, on the one hand, OP and ET films presented the same mass loss as the TT films at each time point, suggesting that the studied activation treatments do not affect the PLLA degradation since they act at the outermost layers of the surface. On the other hand, SH films presented a slightly faster degradation rate than the TT films resulting probably from the greater surface in contact with the NaOH solution, due to its higher roughness. Finally, TT, OP, and ET films showed a degradation rate statistically similar to the REMEDY stent degradation rate. Associating this result with the high mechanical properties of TT films and the unaltered crystallinity and Mw after plasma and enzyme hydrolysis, it can be concluded that the TT, OP, and ET films are suitable for stent fabrication.

According to the SEM images, a clear degradation of the surface and an increased roughness can be observed for all the samples, except for the REMEDY stent surface. The faster degradation observed by a mass loss on SC compared to the other samples was confirmed by a higher surface deterioration, and an increase of Ra by a factor of 5.51. Surfaces with a thermal treatment presented a lower surface degradation and Ra was increased by a factor 1.86. Therefore, confirming that the increase of crystallinity made the PLLA more resistant to degradation. This effect was also confirmed with the REMEDY stent which did not start the degradation, after 10 days of immersion in NaOH, due to the high percentage of crystallinity. The NaOH, plasma, and enzyme activated surfaces had a surface degradation similar to TT, confirming also that the studied activation treatments did not affect PLLA degradation.

3.4. HUVECs Adhesion

In order to biologically characterize the effect of plasma, NaOH, and enzyme hydrolysis of PLLA solvent-cast films, HUVECs adhesion was evaluated after 12 h of cell culture. The cell number was slightly higher on SH films (25,787 $\pm$ 2288 cells/cm^2) compared to the TT surfaces (21,297 $\pm$ 1528 cell/cm^2) (Figure 6a). Whereas, OP and ET films presented a statistically higher number of HUVECs, 36,958 $\pm$ 2967 and 33,541 $\pm$ 4434 cells/cm^2, respectively, compared to the TT and SH samples. SEM images visually confirmed the higher cell density on the activated surfaces and showed a higher spreading on these surfaces compared to the TT films (Figure 7). In particular, high magnification images of the TT surfaces showed round HUVECs, non-expanded, showing an initial adhesion stage with many extended *filopodia*. The low cell affinity of the TT surfaces was expected since PLLA is chemically inert with no reactive side-chain groups that could accelerate cell spreading. On the contrary, HUVECs on OP, SH, and ET films were flat and extended. This higher cell number and spreading on the activated surfaces induced a percentage of area occupied by HUVECs at least four times higher compared to the TT samples (Figure 6b). The plasma and enzyme activation had the highest and statistical equal values with 66.0 $\pm$ 11.5 and 58.7 $\pm$ 3.9%, respectively. Surface characteristics such as wettability and functional group density evolved proportionally with the HUVECs adhesion on the three functionalized surfaces, confirming the relationship between the higher functional group densities, hydrophilicity and increased cell adhesion. The reason for this correlation could be attributed to higher protein adsorption on the hydrophilic surfaces, as reported previously [64,65].

In summary, concerning the effect of the different activation treatments applied to the PLLA surfaces on the cell response we found that, on the one hand, plasma and enzyme activation increased PLLA biocompatibility by improving HUVECs adhesion and also, created a higher density of surface functional groups that can be used to covalently immobilize biomolecules. On the other hand, sodium hydroxide activation showed a lower density of the activated functional groups on the surface compared to other activation treatments and HUVECs adhesion slightly increased compared to the control. Moreover, the NaOH activation increased the PLLA films roughness, which could dramatically induce a higher platelet adhesion and promote thrombus formation when using this surface for cardiovascular applications [66,67].

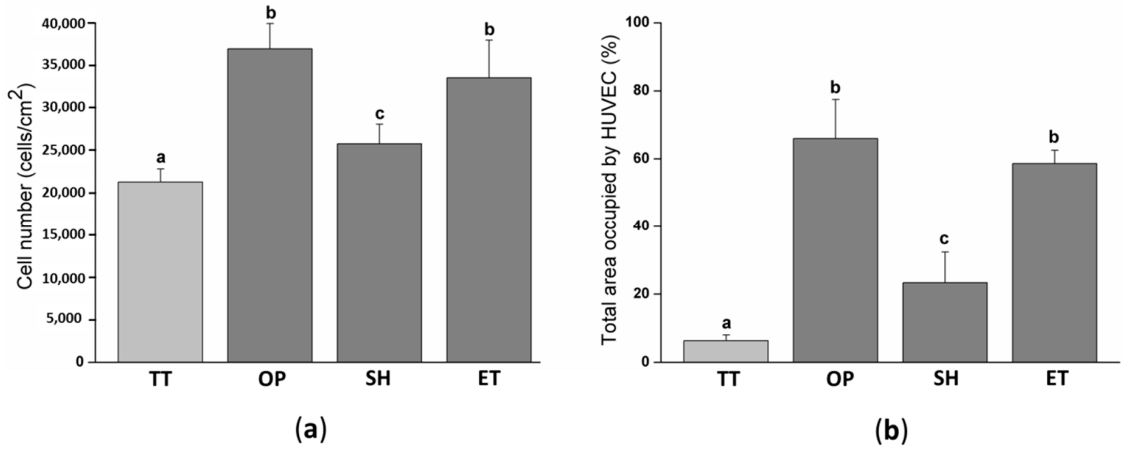

Figure 6. HUVECs adhesion and spreading on TT and activated films after 12 h of cell culture: (**a**) Cell number quantified by the Lactate Dehydrogenase LDH enzymatic assay; (**b**) percent of area occupied by HUVEC obtained after the SEM images analysis. Images were analyzed with the FIJI software. Columns with different letters belong to statistically different groups (p-value < 0.05). **TT**: Thermally treated solvent casting films; **OP**: Oxygen plasma TT films; **SH**: Sodium hydroxide etched TT films; **ET**: Enzyme treated TT films.

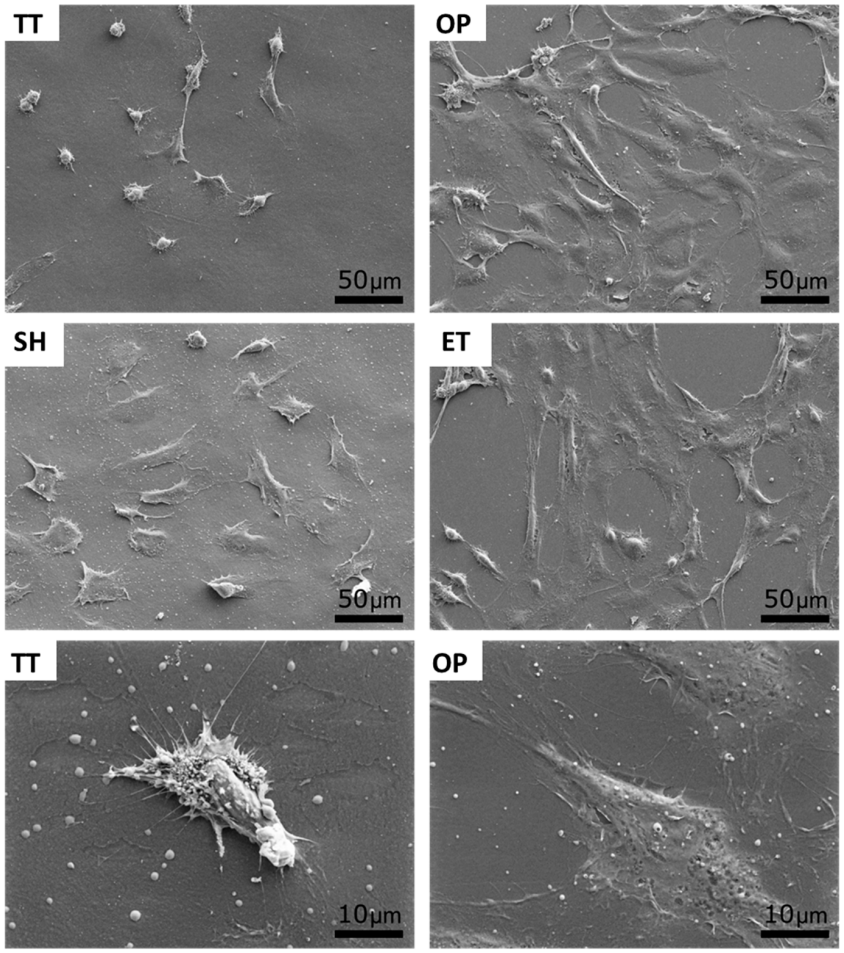

Figure 7. SEM images of HUVECs adhesion and spreading on TT and activated surfaces after 12 h of incubation. Bottom images show a high magnification a low spread cell (TT) and a highly spread cell (OP). **TT**: Thermally treated films; **OP**: Oxygen plasma TT films; **SH**: Sodium hydroxide etched TT films; **ET**: Enzyme treated TT films.

3.5. BRS Obtained by the Solvent-Cast Direct Write Technique

The solvent-cast high molecular weight PLLA activated with plasma or enzymes presented an appropriate crystallinity, molecular weight, degradation rate, and enhanced ECs response which makes it a biomaterial suitable to be used for BRS fabrication. As a proof of concept, PLLA BRS stents were fabricated by the solvent-cast direct-write technique to assess its feasibility. Tubular structures of 5 mm diameter and 20 mm length (Figure 8) were obtained. Perfectly regular and seamless stent structures were obtained, with a regular monofilament diameter of ≈150 µm. The junctions were properly welded leading to a flexible and resistant prototype.

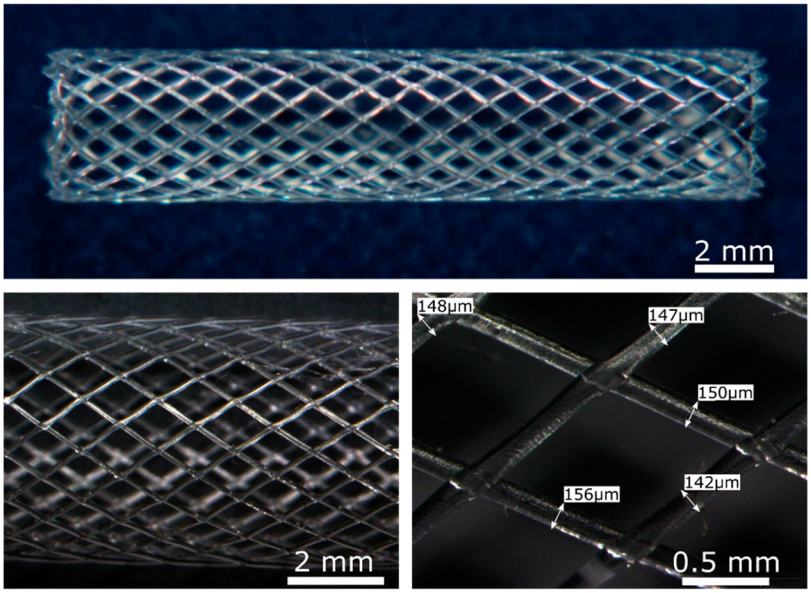

Figure 8. PLLA BRS obtained by the solvent-cast direct-write technique. Upper image: General image of PLLA BRS by optical microscopy. Lower images: Detailed optical microscopy images of the PLLA BRS struts.

The stent design, following a rhombohedral pattern, was selected in order to obtain a welded structure with appropriate mechanical properties to expand and deploy into the artery. The design should ideally minimize the quantity of material in contact with the blood stream to avoid blood turbulence, as this may lead to LST. Moreover, its design also plays a role in its degradation rate. The in vitro degradation rate of a device is affected by several factors such as the material composition, pH, molecular weight, or device geometry, etc. Since the experimental research for an optimal device can be time-consuming, mathematical models of interest regarding the in vitro degradation rate of devices can be found in the literature [68]. The degradation of PLLA consists first, in a chemical hydrolysis where water breaks the hydrolysable bonds and secondly, the resulting degradation products are removed by the organism. The previous considerations allow introducing the concept of safe-by-design to our stent in order to minimize the risk of the polymeric nano-biomaterials degradation products of PLLA when delivered in the bloodstream and enhancing the device safety [68,69].

4. Conclusions

PLLA is a biodegradable polymer with no reactive side-chain groups making its surface modifications a challenging task. In this work, we evaluate the potential of the solvent-cast PLLA functionalized by oxygen plasma, NaOH solution, or cutinase enzymes to enhance ECs adhesion and to be used for 3D printed BRS fabrication. Solvent casting of PLLA with chloroform leaves residues on the surface inducing cytotoxicity of the material and obtaining a low crystallinity and mechanical properties (i.e., Young's modulus and

UTS). After the thermal treatment, solvent-cast PLLA presented full biocompatibility, increased mechanical properties, and degradation rates similar to the commercial REMEDY BRS. It was characterized the quantity and effectiveness of surface functional groups obtained after chemical hydrolysis of ester bonds or by grafting of reactive species, obtained by oxygen plasma, with the polymer chains. The plasma and enzyme functionalization did not affect the physical properties of 2D planar PLLA surfaces, such as crystallinity or degradation, or significantly increase their hydrophilicity and the density of surface functional groups, which reverted in enhanced ECs adhesion and spreading. On the contrary, NaOH etching induced surface roughness and was proven to be less efficient than the plasma and enzymes in terms of creating functional groups and improving the ECs response. The solvent cast direct writing technique allowed the seamless 3D printing of PLLA BRS. Consequently, the combined use of the solvent cast direct writing technique and plasma or enzyme functionalization holds great potential to fabricate 3D printed PLLA BRS with the capacity to accelerate the surface endothelialization.

Author Contributions: Conceptualization, R.S., C.C. (Cristina Caparrós), C.C. (Cristina Canal), and M.P.; methodology, R.S. and M.P.; software, R.S.; validation, R.S., C.C. (Cristina Caparrós), and R.S.; formal analysis, R.S. and C.C. (Cristina Caparrós); investigation, R.S., C.C. (Cristina Caparrós), and Y.R.; resources, J.B., E.H.A., and G.M.G.; data Curation, R.S.; writing—original draft preparation, R.S.; writing—review and editing, R.S. and M.P.; visualization, R.S. and M.P.; supervision, C.C. (Cristina Caparrós), C.C. (Cristina Canal), and M.P.; project administration, M.P.; funding acquisition, C.C. (Cristina Caparrós), C.C. (Cristina Canal), and M.P. All authors have read and agreed to the published version of the manuscript.

Funding: This work was supported by the Spanish Government for financial support through project RTI2018-67183-R (MINECO/FEDER). Authors acknowledge the Agency for Administration of University and Research Grants of the Government of Catalonia (2017SGR-1165), and the project (BASE3D 001-P-001646) co-financed by the European Union Regional Development Fund within the framework of the ERDF Operational Program of Catalonia 2014–2020 with a grant of 50% of the total cost eligible and MINECO for PID2019-103892RB-I00 project. R.S. acknowledges the Erasmus Mundus Doctoral Programme DocMASE of the European Commission (FPA 2011 0020).

Acknowledgments: Authors acknowledge Montse Domínguez Escalante for helping in the XPS measurement and analysis and Trifon Todorov Trifonov for helping in the SEM measurement and analysis.

Conflicts of Interest: The authors declare no conflict of interest. The funders had no role in the design of the study; in the collection, analyses, or interpretation of data; in the writing of the manuscript, or in the decision to publish the results.

References

1. Nakamura, K.; Keating, J.H.; Edelman, E.R. Pathology of Endovascular Stents. *Interv. Cardiol. Clin.* **2016**, *5*, 391–403. [CrossRef] [PubMed]
2. Garg, S.; Serruys, P.W. Coronary stents: Looking forward. *J. Am. Coll. Cardiol.* **2010**, *56*, 43–78. [CrossRef]
3. Gogas, B.D. Bioresorbable scaffolds for percutaneous coronary interventions. *Glob. Cardiol. Sci. Pract.* **2014**, *4*, 409–427. [CrossRef]
4. Suzuki, S.; Ikada, Y. Medical applications. In *Poly (lactic acid): Synthesis, Structures, Properties, Processing and Applications*; Auras, R., Lim, L., Selke, S.E.M., Tsuji, H., Eds.; John Wiley and Sons: Hoboken, NJ, USA, 2010; pp. 445–454.
5. Farah, S.; Anderson, D.G.; Langer, R. Physical and mechanical properties of PLA, and their functions in widespread applications—A comprehensive review. *Adv. Drug Deliv. Rev.* **2016**, *107*, 367–392. [CrossRef]
6. Ramcharitar, S.; Serruys, P.W. Fully biodegradable coronary stents: Progress to date. *Am. J. Cardiovasc. Drugs* **2008**, *8*, 305–314. [CrossRef]
7. Wykrzykowska, J.J.; Kraak, R.P.; Hofma, S.H.; Van Der Schaaf, R.J.; Koch, K.T.; Baan, J.; Vis, M.M. Bioresorbable Scaffolds versus Metallic Stents in Routine. *N. Engl. J. Med.* **2017**, *376*, 2319–2328. [CrossRef]
8. Cassese, S.; Byrne, R.A.; Ndrepepa, G.; Kufner, S.; Wiebe, J.; Repp, J.; Schunkert, H.; Fusaro, M. Everolimus-eluting bioresorbable vascular scaffolds versus everolimus-eluting metallic stents: A meta-analysis of randomized controlled trials. *Lancet.* **2015**, *6736*, 1–8. [CrossRef]
9. Lipinski, M.J.; Escarcega, R.O.; Baker, N.C.; Benn, H.A.; Gaglia, M.A.; Torguson, R.; Waksman, R. Scaffold Thrombosis After Percutaneous Coronary Intervention with ABSORB Bioresorbable Vascular Scaffold. *JACC Cardiovasc. Interv.* **2016**, *9*, 12–24. [CrossRef] [PubMed]

10. Nazneen, F.; Herzog, G.; Arrigan, D.W.M.; Caplice, N.; Benvenuto, P.; Galvin, P.; Thompson, M. Surface chemical and physical modification in stent technology for the treatment of coronary artery disease. *J. Biomed. Mater. Res. B Appl. Biomater.* **2012**, *100*, 1989–2014. [CrossRef] [PubMed]
11. Schieber, R.; Lassarre, F.; Hans, M.; Fernandez-Yague, M.; Diaz-Ricart, M.; Escolar, G.; Ginebra, M.-P.; Mucklich, F.; Pegueroles, M. Direct Laser Interference Patterning of CoCr Alloy Surfaces to Control Endothelial Cell and Platelet Response for Cardiovascular Applications. *Adv. Healthc. Mater.* **2017**, *6*, 1700327. [CrossRef]
12. Att, W.; Hori, N.; Iwasa, F.; Yamada, M.; Ueno, T.; Ogawa, T. The effect of UV-photofunctionalization on the time-related bioactivity of titanium and chromium-cobalt alloys. *Biomaterials* **2009**, *30*, 4268–4276. [CrossRef]
13. Koo, G.-H.; Jang, J. Surface modification of poly (lactic acid) by UV/Ozone irradiation. *Fibers Polym.* **2009**, *9*, 674–678. [CrossRef]
14. Carpenter, J.; Khang, D.; Webster, T.J. Nanometer polymer surface features: The influence on surface energy, protein adsorption and endothelial cell adhesion. *Nanotechnology* **2008**, *19*, 505103. [CrossRef]
15. Sun, T.; Tan, H.; Han, D.; Fu, Q.; Jiang, L. No platelet can adhere-largely improved blood compatibility on nanostructured superhydrophobic surfaces. *Small* **2005**, *1*, 959–963. [CrossRef] [PubMed]
16. De Mel, A.; Jell, G.; Stevens, M.M.; Seifalian, A.M. Biofunctionalization of biomaterials for accelerated in situ endothelialization: A review. *Biomacromolecules* **2008**, *9*, 2969–2979. [CrossRef] [PubMed]
17. Castellanos, M.I.; Mas-Moruno, C.; Grau, A.; Serra-Picamal, X.; Trepat, X.; Albericio, F.; Joner, M.; Manero, J.M.; Pegueroles, M. Functionalization of CoCr surfaces with cell adhesive peptides to promote HUVECs adhesion and proliferation. *Appl. Surf. Sci.* **2016**, *393*, 82–92. [CrossRef]
18. Nyanhongo, G.S.; Rodríguez, R.D.; Prasetyo, E.N.; Caparrós, C.; Ribeiro, C.; Sencadas, V.; Lanceros-Mendez, S.; Acero, E.H.; Guebitz, G.M. Bioactive albumin functionalized polylactic acid membranes for improved biocompatibility. *React. Funct. Polym.* **2013**, *73*, 1399–1404. [CrossRef]
19. Chen, X.; Sevilla, P.; Aparicio, C. Surface biofunctionalization by covalent co-immobilization of oligopeptides. *Colloids Surf. B Biointerfaces* **2013**, *107*, 189–197. [CrossRef]
20. Chu, P.K.; Chen, J.Y.; Wang, L.P.; Huang, N. Plasma-surface modification of biomaterials. *Mater. Sci. Eng. R Rep.* **2002**, *36*, 143–206. [CrossRef]
21. Siow, K.S.; Britcher, L.; Kumar, S.; Griesser, H.J. Plasma Methods for the Generation of Chemically Reactive Surfaces for Biomolecule Immobilization and Cell Colonization—A Review. *Plasma Process. Polym.* **2006**, *3*, 392–418. [CrossRef]
22. Jordá-Vilaplana, A.; Fombuena, V.; García-García, D.; Samper, M.D.; Sánchez-Nácher, L. Surface modification of polylactic acid (PLA) by air atmospheric plasma treatment. *Eur. Polym. J.* **2014**, *58*, 23–33. [CrossRef]
23. Miller, D.C.; Thapa, A.; Haberstroh, K.M.; Webster, T.J. Endothelial and vascular smooth muscle cell function on poly (lactic-co-glycolic acid) with nano-structured surface features. *Biomaterials* **2004**, *25*, 53–61. [CrossRef]
24. Serrano, M.C.; Portolés, M.T.; Vallet-Regí, M.; Izquierdo, I.; Galletti, L.; Comas, J.V.; Pagani, R. Vascular endothelial and smooth muscle cell culture on NaOH-treated poly(epsilon-caprolactone) films: A preliminary study for vascular graft development. *Macromol. Biosci.* **2005**, *5*, 415–423. [CrossRef] [PubMed]
25. Pellis, A.; Herrero Acero, E.; Ferrario, V.; Ribitsch, D.; Guebitz, G.M.; Gardossi, L. The Closure of the Cycle: Enzymatic Synthesis and Functionalization of Bio-Based Polyesters. *Trends Biotechnol.* **2016**, *34*, 316–328. [CrossRef] [PubMed]
26. Pellis, A.; Silvestrini, L.; Scaini, D.; Coburn, J.M.; Kaplan, D.L.; Herrero, E.; Guebitz, G.M. Enzyme-catalyzed functionalization of poly (L-lactic acid) for drug delivery application. *Process Biochem.* **2016**, 1–20. [CrossRef]
27. Tham, C.Y.; Abdul Hamid, Z.A.; Ahmad, Z.; Ismail, H.A. Surface Engineered Poly (lactic acid) (PLA) Microspheres by Chemical Treatment for Drug Delivery System. *Key Eng. Mater.* **2014**, *594*, 214–218. [CrossRef]
28. Tsuji, H.; Ikada, Y. Properties and Morphology of Poly (L -lactide) II. Hydrolysis in Alkaline Solution. *J. Polym. Sci. Part A Polym. Chem.* **1997**, *36*, 59–66. [CrossRef]
29. Shishoo, R. Plasma Treatment—Industrial Applications and Its Impact on the C & L Industry. *J. Coat. Fabr.* **1996**, *26*, 26–35.
30. Rasal, R.M.; Janorkar, A.V.; Hirt, D.E. Progress in Polymer Science Poly (lactic acid) modifications. *Prog. Polym. Sci.* **2010**, *35*, 338–356. [CrossRef]
31. Pellis, A.; Acero, E.H.; Weber, H.; Obersriebnig, M.; Breinbauer, R.; Srebotnik, E.; Guebitz, G.M. Biocatalyzed approach for the surface functionalization of poly (L-lactic acid) films using hydrolytic enzymes. *Biotechnol. J.* **2015**, *10*, 1739–1749. [CrossRef]
32. Guo, S.Z.; Gosselin, F.; Guerin, N.; Lanouette, A.M.; Heuzey, M.C.; Therriault, D. Solvent-cast three-dimensional printing of multifunctional microsystems. *Small* **2013**, *9*, 4118–4122. [CrossRef]
33. Heng, B.C.; Bezerra, P.P.; Meng, Q.R.; Chin, D.W.-L.; Koh, L.B.; Li, H.; Zhang, H.; Preiser, P.R.; Boey, F.Y.-C.; Venkatraman, S.S. Adhesion, proliferation, and gene expression profile of human umbilical vein endothelial cells cultured on bilayered polyelectrolyte coatings composed of glycosaminoglycans. *Biointerphases* **2010**, *5*, 53–62. [CrossRef]
34. Andukuri, A.; Minor, W.P.; Kushwaha, M.; Anderson, J.M.; Jun, H.-W. Effect of endothelium mimicking self-assembled nanomatrices on cell adhesion and spreading of human endothelial cells and smooth muscle cells. *Nanomedicine* **2010**, *6*, 289–297. [CrossRef] [PubMed]
35. Byun, Y.; Whiteside, S.; Thomas, R.; Dharman, M.; Hughes, J.; Carolina, S. The Effect of Solvent Mixture on the Properties of Solvent Cast Polylactic Acid (PLA) Film. *J. Appl. Polym. Sci.* **2011**, 3577–3582. [CrossRef]
36. Buxadera-Palomero, J.; Canal, C.; Torrent-Camarero, S.; Garrido, B.; Javier Gil, F.; Rodríguez, D. Antifouling coatings for dental implants: Polyethylene glycol-like coatings on titanium by plasma polymerization. *Biointerphases* **2015**, *10*, 29505. [CrossRef]

37. American Society for Testing and Materials International. *Standard Test Method for Transition Temperatures and Enthalpies of Fusion and Crystallization of Polymers by Differential Scanning*; ASTM D3418—03: West Conshohocken, PA, USA, 2003.
38. Fischer, E.W.; Sterzel, H.J.; Wegner, G. Investigation of the structure of solution grown crystals of lactide copolymers by means of chemical reactions. *Kolloid Z. Z. Polym.* **1973**, *251*, 980–990. [CrossRef]
39. Zhai, W.; Ko, Y.; Zhu, W.; Wong, A.; Park, C.B. A study of the crystallization, melting, and foaming behaviors of polylactic acid in compressed CO2. *Int. J. Mol. Sci.* **2009**, *10*, 5381–5397. [CrossRef]
40. American Society for Testing and Materials International. *Standard Test Method for Tensile Properties of Thin Plastic Sheeting*; ASTM D882—02: West Conshohocken, PA, USA, 2002.
41. American Society for Testing and Materials International. *Standard Practice for Cutting Film and Sheeting Test Specimens*; ASTM D6287—98: West Conshohocken, PA, USA, 1998.
42. International Organization for Standardization. *Biological Evaluation of Medical Devices. Part 5: Citotoxicity In Vitro Assays*; ISO 10993-5: Geneva, Switzerland, 2009.
43. Owens, D.K.; Wendt, R.C. Estimation of the surface free energy of polymers. *J. Appl. Polym. Sci.* **1969**, *13*, 1741–1747. [CrossRef]
44. Cam, D.; Hyon, S.; Ikada, Y. Degradation of high molecular weight poly(l-lactide) in alkaline medium. *Biomaterials* **1995**, *16*, 833–843. [CrossRef]
45. Vasanthan, N.; Ly, O. Effect of microstructure on hydrolytic degradation studies of poly (l-lactic acid) by FTIR spectroscopy and differential scanning calorimetry. *Polym. Degrad. Stab.* **2009**, *94*, 1364–1372. [CrossRef]
46. Schindelin, J.; Arganda-Carreras, I.; Frise, E.; Kaynig, V.; Longair, M.; Pietzsch, T.; Preibisch, S.; Rueden, C.; Saalfeld, S.; Schmid, B.; et al. An open source platform for biological image analysis. *Nat. Methods* **2012**, *9*, 676–682. [CrossRef] [PubMed]
47. Salama, A.F.; Tousson, E.; Shalaby, K.A.F.; Hussien, H.T. Protective effect of curcumin on chloroform as by-product of water chlorination induced cardiotoxicity. *Biomed. Prev. Nutr.* **2014**, *4*, 225–230. [CrossRef]
48. Fang, C.; Behr, M.; Xie, F.; Lu, S.; Doret, M.; Luo, H.; Yang, W.; Aldous, K.; Ding, X.; Gu, J. Mechanism of chloroform-induced renal toxicity: Non-involvement of hepatic cytochrome P450-dependent metabolism. *Toxicol. Appl. Pharmacol.* **2008**, *227*, 48–55. [CrossRef]
49. Rhim, J.-W.; Mohanty, A.K.; Singh, S.P.; Ng, P.K.W. Effect of the processing methods on the performance of polylactide films: Thermocompression versus solvent casting. *J. Appl. Polym. Sci.* **2006**, *101*, 3736–3742. [CrossRef]
50. Hsu, S.; Yao, Y.L. Effect of Film Formation Method and Annealing on Crystallinity of poly (L-lactic acid) films. In Proceedings of the ASME 2011 International Manufacturing Science and Engineering Conference, Corvallis, OR, USA, 13–17 June 2011.
51. Weir, N.A.; Buchanan, F.J.; Orr, J.F.; Farrar, D.F.; Boyd, A. Processing, annealing and sterilisation of poly-L-lactide. *Biomaterials* **2004**, *25*, 3939–3949. [CrossRef] [PubMed]
52. Perego, G.; Cella, G.; Bastioli, C. Effect of molecular weight and crystallinity on poly (lactic acid) mechanical properties. *J. Appl. Polym. Sci.* **1996**, *59*, 37–43. [CrossRef]
53. Van de Velde, K.; Kiekens, P. Biopolymers: Overview of several properties and consequences on their applications. *Polym. Test.* **2002**, *21*, 433–442. [CrossRef]
54. Canal, C.; Gallinetti, S.; Ginebra, M.P. Low-pressure plasma treatment of polylactide fibers for enhanced mechanical performance of fiber-reinforced calcium phosphate cements. *Plasma Process. Polym.* **2014**, *11*, 694–703. [CrossRef]
55. Tkavc, T.; Vesel, A.; Acero, E.H.; Zemljič, L.F. Comparison of oxygen plasma and cutinase effect on polyethylene terephthalate surface. *J. Appl. Polym. Sci.* **2013**, *128*, 3570–3575. [CrossRef]
56. Ribitsch, D.; Acero, E.H.; Greimel, K.; Dellacher, A.; Zitzenbacher, S.; Marold, A.; Rodriguez, R.D.; Steinkellner, G.; Gruber, K.; Schwab, H.; et al. A new esterase from Thermobifida halotolerans hydrolyses polyethylene terephthalate (PET) and polylactic acid (PLA). *Polymers* **2012**, *4*, 617–629. [CrossRef]
57. Hirotsu, T.; Nakayama, K.; Tsujisaka, T.; Mas, A.; Schue, F. Plasma surface treatments of melt-extruded sheets of poly (L-lactic acid). *Polym. Eng. Sci.* **2002**, *42*, 299–306. [CrossRef]
58. Pio, T.F.; Macedo, G.A. Optimizing the production of cutinase by Fusarium oxysporum using response surface methodology. *Enzyme Microb. Technol.* **2007**, *41*, 613–619. [CrossRef]
59. Li, S. Hydrolytic degradation characteristics of aliphatic polyesters derived from lactic and glycolic acids. *J. Biomed. Mater. Res.* **1999**, *48*, 342–353. [CrossRef]
60. Oberhauser, J.P.; Hossainy, S.; Rapoza, R.J. Design principles and performance of bioresorbable polymeric vascular scaffolds BVS ABSORB Cohort B device. *EuroIntervention* **2009**, *5*, 15–22. [CrossRef]
61. Middleton, J.C.; Tipton, A.J. Synthetic Biodegradable Polymers as orthopedic devices. *Biomaterials* **2000**, *21*, 2335–2346. [CrossRef]
62. Onuma, Y.; Serruys, P.W. Bioresorbable scaffold: The advent of a new era in percutaneous coronary and peripheral revascularization. *Circulation* **2011**, *123*, 779–797. [CrossRef]
63. Delabarde, C.; Plummer, C.J.G.; Bourban, P.E.; Månson, J.A.E. Accelerated ageing and degradation in poly-L-lactide/hydroxyapatite nanocomposites. *Polym. Degrad. Stab.* **2011**, *96*, 595–607. [CrossRef]
64. Arima, Y.; Iwata, H. Effect of wettability and surface functional groups on protein adsorption and cell adhesion using well-defined mixed self-assembled monolayers. *Biomaterials* **2007**, *28*, 3074–3082. [CrossRef]
65. Shah, A.; Shaha, S.; Mani, G.; Wenke, J.; Agrawal, C.M. Endothelial cell behaviour on gas-plasma-treated PLA surfaces: The roles of surface chemistry and roughness. *J. Tissue Eng. Regen. Med.* **2011**, *5*, 301–312. [CrossRef] [PubMed]

66. Park, J.Y.; Gemmell, C.H.; Davies, J.E. Platelet interactions with titanium: Modulation of platelet activity by surface topography. *Biomaterials* **2001**, *22*, 2671–2682. [CrossRef]
67. Hecker, J.F.; Scandrett, L.A. Roughness and thrombogenicity of the outer surfaces of intravascular catheters. *J. Biomed. Mater. Res.* **1985**, *19*, 381–395. [CrossRef] [PubMed]
68. Casalini, T. Bioresorbability of polymers: Chemistry, mechanisms, and modeling. In *Bioresorbable Polymers for Biomedical Applications: From Fundamentals to Translational Medicine*; Perale, G., Hilborn, J., Eds.; Woodhead Publishing: Sawston, UK, 2017; pp. 65–83.
69. Borchard, G.; Som, C.; Zinn, M.; Ostafe, V.; Borges, O.; Perale, G.; Wick, P. Polymeric nano-biomaterials for medical applications: Advancements in developing and implementation considering safety-by-design concepts. *Front. Bioeng. Biotechnol.* **2020**, *8*, 1–2. [CrossRef] [PubMed]